Void Fraction Influence Over Aqueous Foam Flow: Wall Shear Stress and Core Shear Evolution

Rogelio Chovet, Fethi Aloui

HAL Id: hal-03579829
https://hal-uphf.archives-ouvertes.fr/hal-03579829

Submitted on 16 Aug 2022

Void Fraction Influence Over Aqueous Foam Flow: Wall Shear Stress and Core Shear Evolution

Rogelio Chovet and Fethi Aloui

Abstract In this study, the two main transport characterization problems of the foam flow are studied: foam flow stability, through the evolution of the velocity at the core of the foam, and rheology, with the study of the wall shear stress over the lateral walls, for different void fractions. The same velocity profile (block flow, mean velocity 1.75 cm/s) is imposed to the foam flow, at the inlet of the channel, for several void fractions (air/water relation) going from 55 to 85 %. Later on these ones are passed through a singularity (fence) to study the different behaviours induced by the particular properties of each case. The velocity fields, the lateral liquid film thickness and the lateral wall shear stress fields are obtained and compared with one another to comprehend and remark the difference in such a complex flow. The results show that as we move closer to very dry foams the shear at the foam core increases and its velocity becomes higher. However, the wall shear stress at the lateral wall does not present big deviations from one void fraction to the other.

Nomenclature

e	Film thickness
$\vec{e}_x$	Unit vector in the x-coordinate direction
Q_g	Gas flow rate
Q_l	Liquid flow rate
Q_t	Total foam flow rate
u	Axial velocity component

R. Chovet • F. Aloui (✉)

LAMIH CNRS UMR 8201, Department of Mechanics, University of Valenciennes et du Hainaut-Cambrésis (UVHC), Campus Le Mont Houy, Valenciennes Cedex 9 59313, France

e-mail: Rogelio.Chovet@gmail.com; Fethi.Aloui@univ-valenciennes.fr

$\vec{u}$	Axial velocity vector component
v	Vertical velocity component
x	Axial axe direction
y	Vertical axe direction
z	Depth axe direction

Greek Letters

β	Quality (foam void fraction)
τ	Wall shear stress
μ_l	Dynamic viscosity of the liquid phase

Abbreviation

PIV   Particle image velocimetry

66.1 Introduction

Since the beginning of the twentieth century we have been experiencing a phenomenon that has changed the way we look at energy. Exponential human population opened the mind of the scientific community and created a movement whose only purpose is to innovate topics related to all fields of energy (from creation to consumption). One of many original ideas is the use of "not-regular" fluids over "regular" applications to improve the efficiency of these ones. Foam studies have been around since 1887, when Lord Kelvin exposed the packing and structure of the ideal bubble to bubble configuration. Nowadays, due to the energy challenge we are facing, people start to take into consideration this kind of fluids to improve industrial processes. Its unusual rheology properties, low density and important interfacial surface, gives foam flow many interesting uses: assisted oil extraction and heat exchange, among others.

Aqueous foams are complex fluids made out of a dispersion of gas bubbles in a soapy liquid. These bubbles present a wide distribution of sizes, randomly mixed and arranged. There are at least four length scales at which we can consider the properties of a foam:

- The observer's scale, of the order of metres; the foam has the appearance of a soft, opaque solid.
- The millimeter scale, the bubbles can be distinguished; there are a small number of local geometry rules, which describe how the bubbles pack together to form the foam organization [1].
- The micron scale, which shows how liquid is distributed between the bubbles.

- The nanometer scale, at which the molecular structure of the interfaces appears; the presence of particular molecules, surfactants, which positions themselves at the liquid layer between bubbles, lowers the liquid films energy and makes the foam formation easy.

When treated as a macroscopic system, foam elements undergo no significant thermal fluctuation, by means of which it might explore alternatives to the local minimum of energy in which it finds itself [2]. It is not considered to be in a metastable state, since it continually evolves according to the coarsening process, air exchange between neighbour bubbles [3]. However, this is a very slow process. The foam therefore stays very close to a true equilibrium except where a local topological change may take place.

When the topological structure of the foam is altered, it may be brought to a configuration in which there is a violation of the Plateau's rule by the introduction of a *forbidden* vertex. This configuration dissociates rapidly and a new structure is formed. For a 2D flow, the possibilities are rather simple: The so-called T1 process eliminates the fourfold vertex and forms two threefold ones, while the T2 process is associated with the disappearance of a bubble, also known as coalescence. Both processes are sudden events in which the surface energy of the foam drops abruptly and the energy loss is dissipated as heat (Hutzler et al., 2008) [4]. The bubble rearrangement leads to local shear flow of the liquid inside the foam films, resulting in the dissipation of energy and shear rate-dependent contribution to the macro-scopic stress.

Drainage is described as a phenomenon by which liquid flows out of a foam [5]. It may look to be a relatively straightforward fluid problem dealing with the flow between bubbles, but is instead a very complex one, with length scales ranging from nanometres for surfactant molecules to micrometres for films, to millimetres for bubbles, to centimetres for bulk foams. Two main flow stages can be distinguished: the drainage of the films between the bubbles and then the liquid flows to the centre of the channels towards the Plateau junctions. The flow inside the liquid film is due to several phenomena: the gravity force, the capillarity force and the pressure force between the Plateau regions and the film between the bubbles.

A foam may be classified as a dry or wet foam according to the liquid content, which may be represented by the liquid volume fraction. This ranges from much less than 1 % to about 30 %. At each extreme (the dry and wet limits) the bubbles come together to form a structure which resembles one of the classic idealized paradigms of nature's morphology: the division of cells in the dry limit and the close packing of spheres in the wet limit.

Rheological properties of foams, such as elasticity, plasticity and viscosity play a major role in foam production, transportation and application. If foam is subjected to a small shear stress, it deforms like a soft solid. This response can be character-ized with a visco-elastic modulus. For applied low yield stress the visco-plastic flow sets in. In this regime, foams behave like a shear-thinning fluid. This means that their effective viscosity is a decreasing function of the shear rate [6]. Additional rheological phenomena arise at the contact between the bubbles and the confining

solid walls of a channel [7]. If the surface of the solid wall is smooth enough, the foam tends to slip on the wall over a very thin liquid film. In this case, the velocity of the first layer of bubbles in contact with the wall does not match to what is observed with simple liquids [8]. The rheological properties of foams are complex not only because both elastic and viscous responses are non-linear functions of the applied stress but also because shear localization may occur under certain conditions.

66.2 System Description

The system, comprising a stabilized liquid circuit (water with surfactant) and a gas circuit (pressurized air), is injected into the liquid through a porous media into the horizontal test section. The main straight duct is made in a 3.2 m long transparent Plexiglas with a square section of 21 mm × 21 mm. The measurement section is located at the middle of the duct at 1.3 m from the conducts entry. Figure 66.1 shows the schematic view of the fence located at this part of the duct. This one allows us to study the behaviour of the foam flow when faced against a pattern change and its reorganization once through the singularity [9].

66.3 Measurement Techniques

Foam regimes in straight ducts can be qualified in three groups [10]:

- *One-dimensional flow*: for this regime the flow behaves as a whole, it moves like a block or a piston. The velocity vectors have one uniform axial component in the flow direction:

$$\vec{u} = u \cdot \vec{e}_x = cte \cdot \vec{e}_x \qquad (66.1)$$

- *Two-dimensional flow*: it is obtained when the established flow has an axial velocity component that only depends on the *y-coordinate*:

Fig. 66.1 Lateral view of the fence [dimensions in mm]
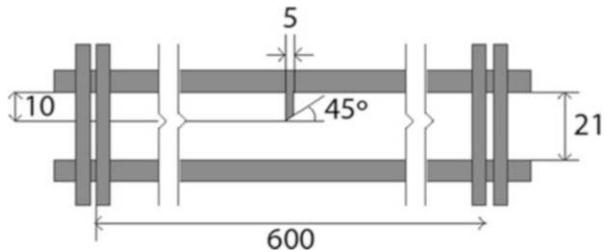
$$\vec{u} = u(y) \cdot \vec{e}_x \tag{66.2}$$

- *Three-dimensional flow*: this one is obtained when the established flow velocity vector presents an axial component that depends on the *z*- and *y-coordinates*:

$$\vec{u} = u(y, z) \cdot \vec{e}_x \tag{66.3}$$

For a foam flow made out of a known gas flow "Q_g" and a known liquid flow "Q_l", we can define the void fraction expression as the measure of the empty space inside the foam:

$$\beta = \frac{Q_g}{Q_t} \tag{66.4}$$

where "Q_t" corresponds to the foam flow such as $Q_t = Q_l + Q_g$.

For our experiments, measurements were undertaken in the first regime (one-dimensional flow regime) using a mean flow velocity of 1.75 cm/s and with a void fraction of 55, 65, 75, and 85 %. The liquid and gas flow rates were measured with a group of rotameters (Brooks).

The particle imaging velocimetry technique was used to obtain the foam flow behaviour, velocity fields and profiles. It is a non-intrusive optic method capable of obtaining the displacement of particles in a plane. This displacement is determined by the comparison of two instantaneous position fields of particles inside. The gas/liquid interface is darker than the rest of the flow. Therefore, the bubbles contour can be used to obtain the movement of the foam flow as a whole. The system used is a TSI set. It uses a software Insight 4G to treat the images. Due to the opacity of the foam flow, the measurements were done for the bubbles flowing over the lateral channel wall. The laser is produced by a double impulsion laser (ND-YAG) with a wavelength of 532 nm (green) and a frequency of 7.25 Hz. Figure 66.2 shows the schematic representation of the setting arrangement [11].
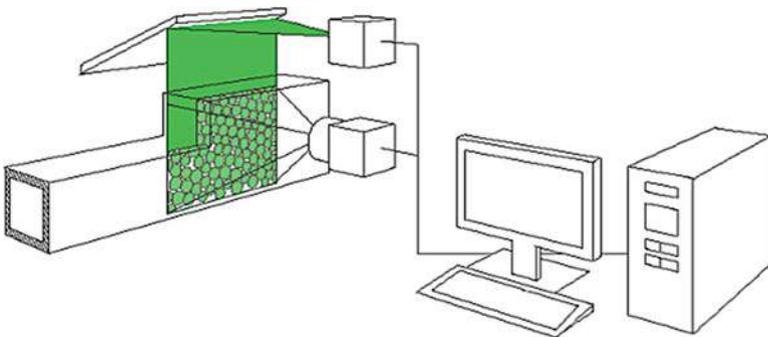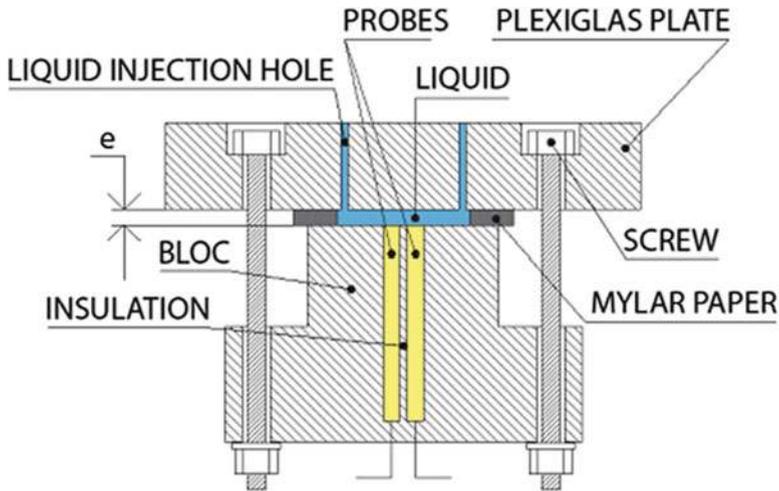

Fig. 66.2 PIV setting arrangement

Fig. 66.3 Calibrate system for the conductimetry probe

The stability experiments conducted were not aimed to accurately locate and determine the T1 and T2 rearrangement. Contrariwise, they were interested in obtaining the velocity changes that these ones may generate in the foam flow and therefore induce a shear over its core. The PIV is a method than can accurately give us these results by analyzing the velocity fields of our foam flow at the wall.

A conductimetry block located at the lateral wall was used to obtain the liquid film thickness evolution. A frequency generator is used to emit a sinusoidal alternating voltage between the conductimetry electrodes (between 50 and 100 kHz) to neglect the electrodes' polarization phenomenon. The block used to measure the liquid film thickness is rigid and cannot be moved. Therefore, to calibrate it, an auxiliary system was created. This circuit is represented in Fig. 66.3. The thickness e between the plate and the block can be adjusted. Then, the liquid fills the space between the plate and the block. The experimental relation gives the output voltage as a function of the thickness e and establishes it for every pair of probes [12].

66.4 Results and Discussion

The two main transport characterization problems (stability and rheology) are undertaken by presenting the results in terms of streamlines, velocity fields and profiles, liquid film thickness evolution over the lateral wall and finally the wall shear stress over the lateral wall for a foam flow with a block velocity of 2 cm/s and a void fraction of 55, 65, 75 and 85 %.
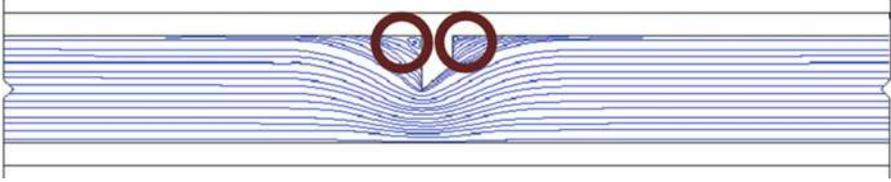
Fig. 66.4 Streamlines of the mean velocity fields
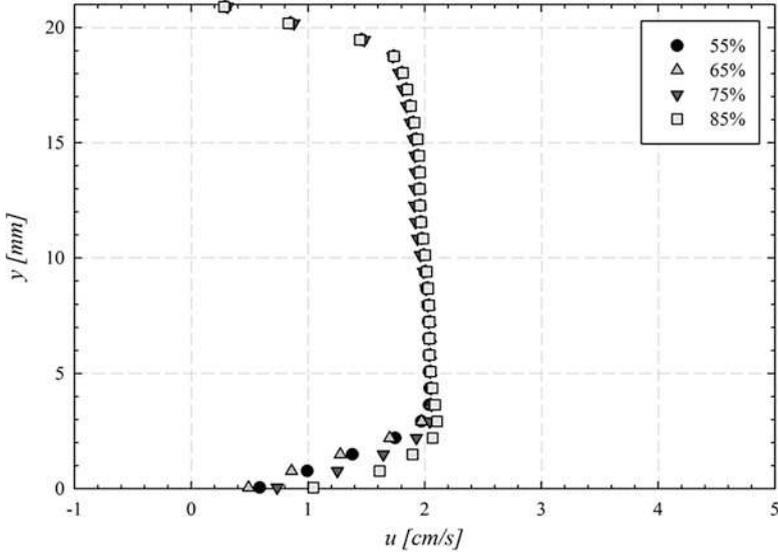

Fig. 66.5 Profile of the axial velocity component upstream of the singularity for all cases

Figure 66.4 shows the streamlines of the mean velocity fields for the foam flowing through the singularity. The presence of the fence causes the formation of dead zones in the immediate vicinity. In these regions the flow becomes slower and it can even get stagnated. In this first approach the foam can be divided in two regions: the principal flow and the dead zones where the bubbles can be completely motionless.

One of the most important aspects of this study was to assure that all foam flows had the exact initial conditions except for the change in the void fraction. This means same bubble size and same velocity profile at the entrance of the conduct. For the bubbles, the same porous medium was used in all cases. It has a porosity of 40 μm and creates bubbles with a diameter of 0.5 mm approximately. Figure 66.5 shows the velocity profile of all cases upstream of the singularity, far away enough to not be influenced by it. It can be seen that they all present the one-dimensional regime with a mean velocity of 1.75 cm/s.
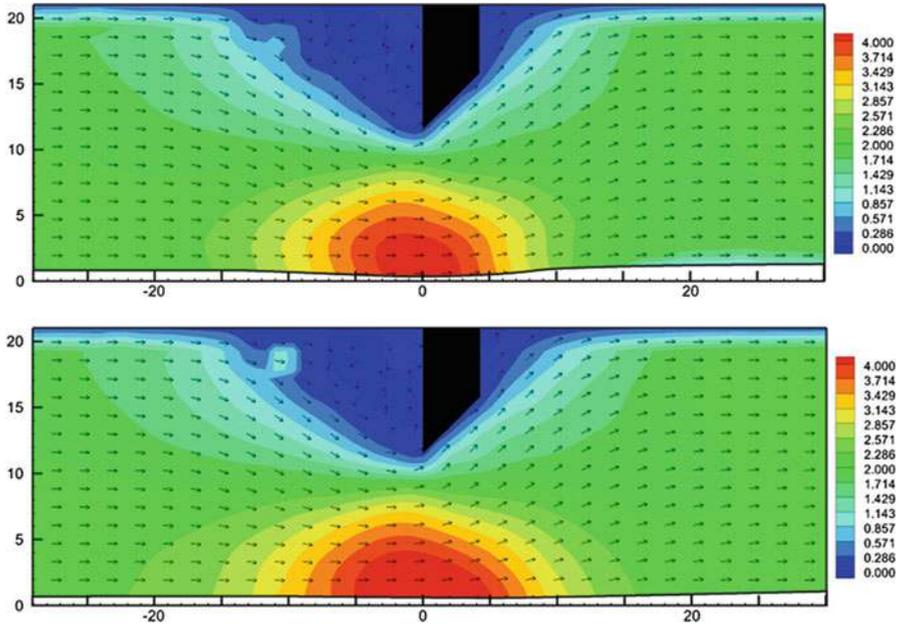
Fig. 66.6 "u" [cm/s] velocity fields for 55 % (*top*) and 85 % (*bottom*)

The "*u*" velocity fields for the void fractions of 55 and 85 % are represented in Fig. 66.6. These two specific cases were selected because they accurately represent the two limits of foam flow, dry and wet limits respectively. Also, in these two images the shear difference it is easily noted. Despite having the same velocity profiles upstream and downstream of the singularity, the velocity fields, while the foam passes through the singularity, are quite different. The dryer foam is more influenced by the singularity than the wet one; it dissipates more energy, in the axial direction, via viscous friction and stores less via its elastic properties. Therefore, it is easier to shear the dryer foam than the wet one. The maximum velocity is achieved for both cases right under the singularity with a value of around 4 cm/s. As the dry foam is more influenced by the velocity it also takes more time to achieve an equilibrium state, around 16 mm for the 11 mm of the wet foam.

The *v* velocity fields for the same void fractions are shown in Fig. 66.7. For both cases, 55% and 85%, the behavior downstream of the singularity is similar. They return to its initial state at about the same distance from the fence. Upstream of the singularity everything changes. Dry foam resists more to change than the wet one. Therefore, dry foam tends to shear less than the wet one. This is due to the gravity effects and the densities differences. Wet foams are denser than dry foams. Therefore, it will be more influenced by the gravitational force. In both cases a maximum value of 1.2 cm/s is obtained at the exit of the singularity and a minimum value of -0.8 at the enter of this one.
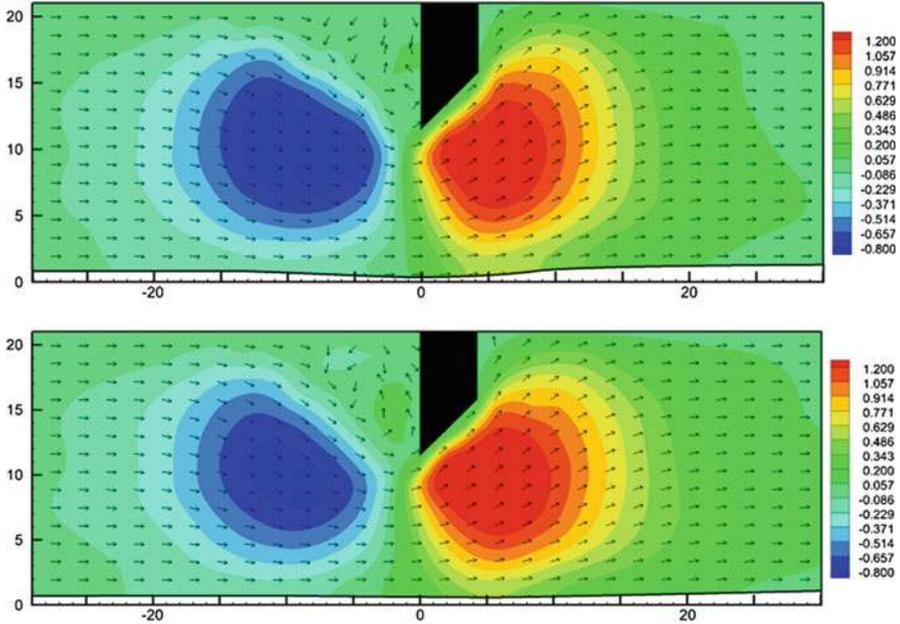
Fig. 66.7 "v" [cm/s] velocity fields for 55 % (*top*) and 85 % (*bottom*)

Figure 66.8 represents the comparison of axial velocity profiles for all cases (55, 65, 75 and 85 %) as they pass though the singularity starting at −25 mm and finishing at 25 mm from it. An acceleration can be remarked as we move closer to the fence ($x = 0$), reaching a maximum velocity of 4.3 cm/s. After this sudden acceleration, the flow returns to equilibrium state with a velocity close to the one it had before entering the singularity. The presence of death zones is clearly noticed near the singularity where the axial velocity tends to 0. The absence of negative velocities indicate that there are no recirculation zones and the foam flow stagnates near the fence. Except for the driest foam (85 %), all other curves present the same appearance putting into evidence once more the facility for the dry foam to shear more than the wet one. This difference is about 15 % in its most deviated points.

Over the same plane the vertical velocity profiles were obtained and they are shown in Fig. 66.9. As in a nozzle, the reduction of the section creates a vertical acceleration towards the passage section below the singularity. As the foam leaves the fence it fully occupies the rest of the duct. This phenomenon is a consequence of its low density and high active surface. At the same time, it gradually decelerates reaching the one-dimensional regime, in which the vertical velocity tends to zero. As for the shear difference, it can be deducted from the velocity profiles that upstream of the singularities wet foam tends to shear more in the vertical direction, due to gravitational forces, than dry foam, and once the obstacle is passed the phenomenon inverses and the dry foam becomes faster and shears more than the

wet foam. Regardless of the different void fractions, the evolution of the mean value of the liquid film over the lateral wall remains approximately the same. As an example, Figure 66.10 shows the instant behaviour of the liquid film thickness for a void fraction of 75 % as bubbles pass over the conductimetry probe. From these signals, the maximum and averaged values are not significant. They are a result of
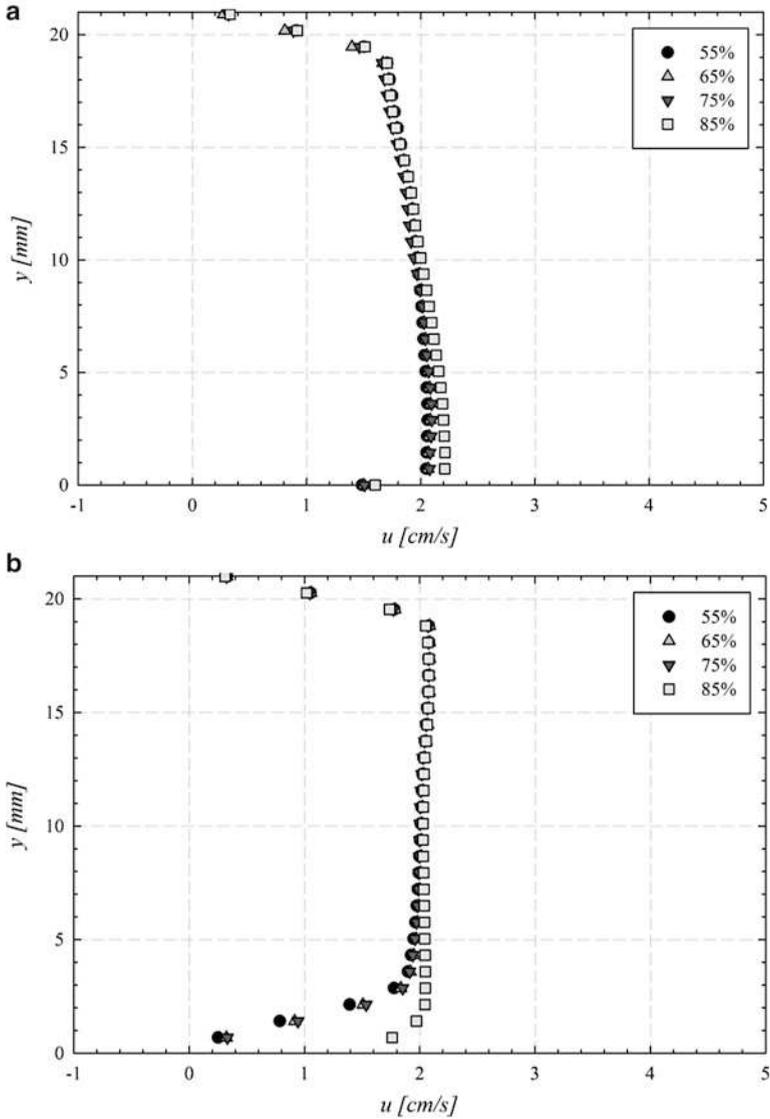

Fig. 66.8 "u" [cm/s] velocity profiles at (**a**) $x=-25$, (**b**) $x=25$, (**c**) $x=-15$, (**d**) $x=15$, (**e**) $x=-5$, (**f**) $x=5$ and (**g**) $x=0$

Fig. 66.8 (continued)
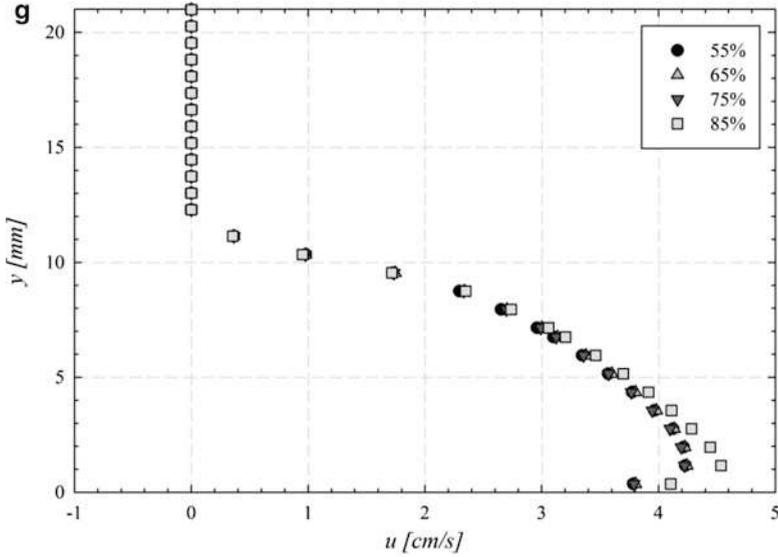
e

f
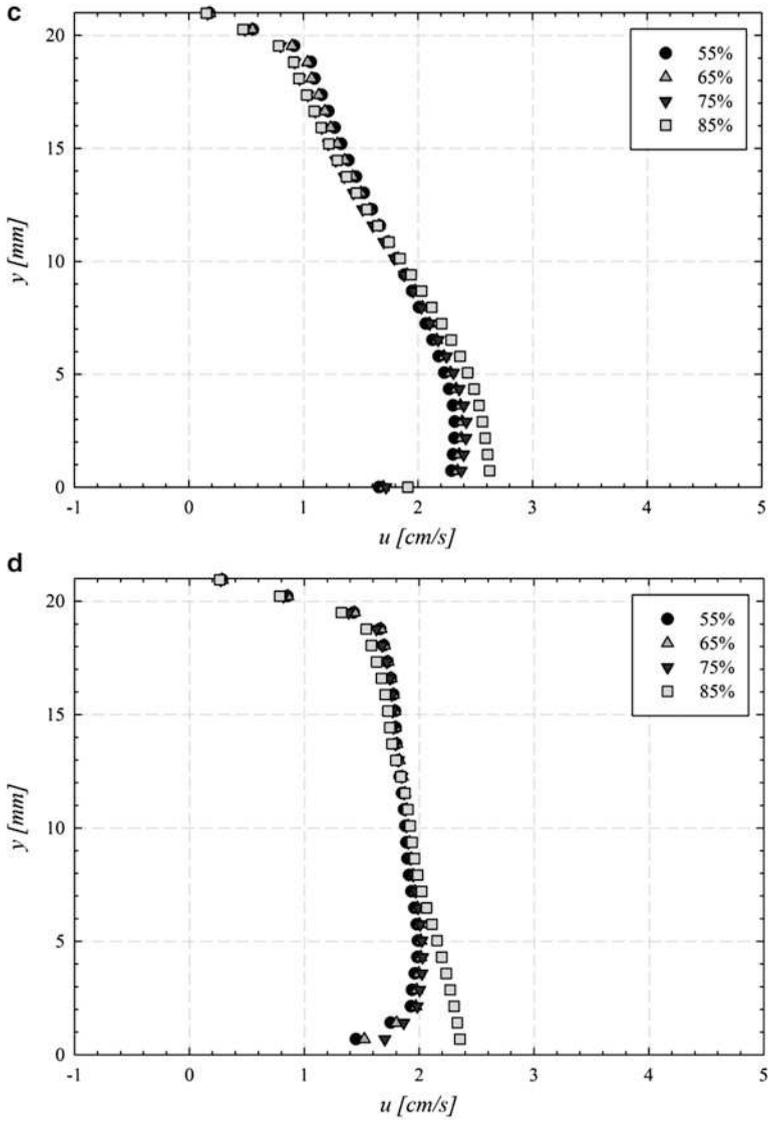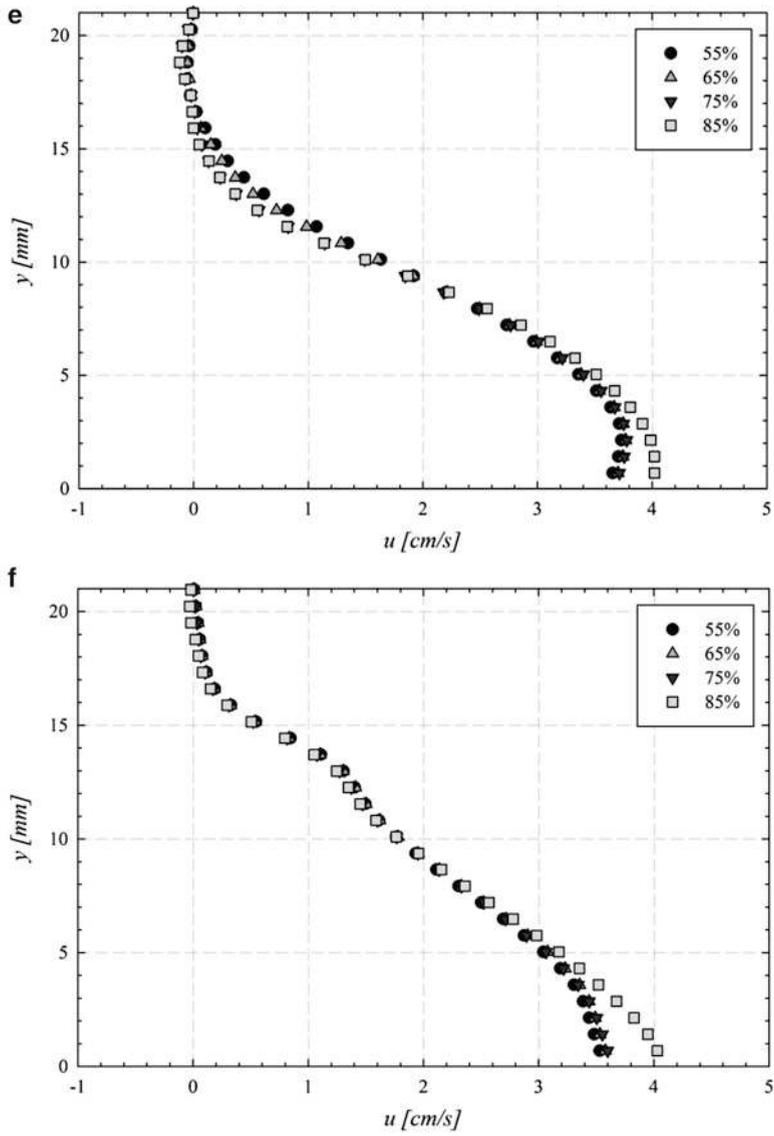
Fig. 66.8 (continued)

Fig. 66.8 (continued)

the passage of a bubble and not the actual conduction of the liquid film. Therefore, only the measurements of the minimal thickness were analyzed.

The evolution of the average liquid film thickness along the lateral wall is represented in Fig. 66.11. It can be noted that, due to the drainage forces (gravity, capillarity and disjoining pressure), the liquid film closest to the bottom of the channel is thicker (around 60 μm) than the one at the top (around 5 μm). Its evolution can be adjusted to a curve with the form $y = 82.33 \times e^{-0.904}$. The thickness of the liquid film at the bottom of the channel depends on the void fraction but does not make part of this study.

Some assumptions were made to calculate the wall shear stress over the lateral wall along the test section: The liquid film thickness remains constant along the axial length, it is equal to the theoretical curve adjusted to the experimental results and the wall velocity gradient is equal to the axial bubble velocity over the wall, shown in Fig. 66.5. The value of the wall shear stress is obtained with the expression

$$\tau(y) = \mu_l \frac{\delta u}{\delta y} \tag{66.5}$$

where $\mu_l = 1.002 \times 10^{-3}$ is the liquid dynamic viscosity (same as the water), δu is the wall velocity gradient and $\delta y = e$ is the thickness of the liquid film.

Figure 66.12 shows the wall shear stress field over the lateral wall for both limits, wet (55 %) and dry (85 %). Though the velocity fields and profiles of the axial component showed us a difference in terms of shear and behaviour of these two

void fractions, the wall shear stress difference is not appreciated. Maximum values are achieved away from singularity at the top of the channel (4 Pa). The axial velocity takes a minor part in the wall shear stress and it is the liquid film thickness that influences the behaviour of this one the most. Therefore, in those places where the liquid film tends to a minimum value (5 μm) the wall shear stress tilts to its maximum.
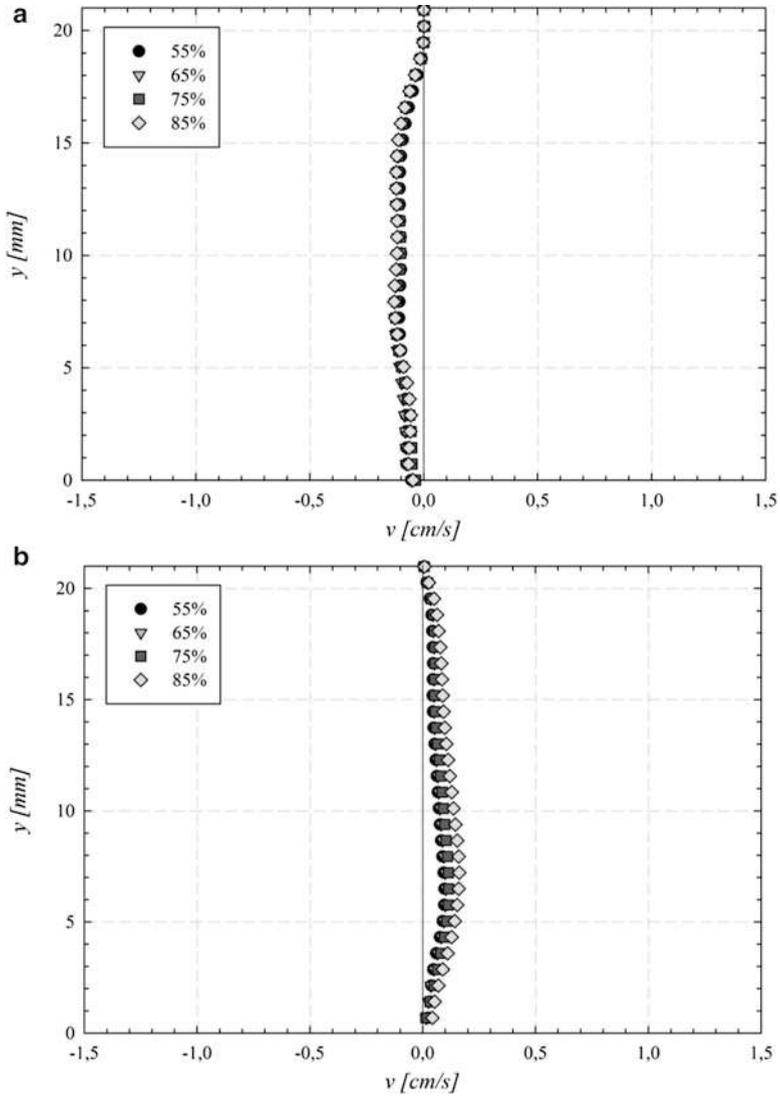

Fig. 66.9 "v" [cm/s] velocity profiles at (**a**) $x=-25$, (**b**) $x=25$, (**c**) $x=-15$, (**d**) $x=15$, (**e**) $x=-5$, (**f**) $x=5$ and (**g**) $x=0$

c

d

Fig. 66.9 (continued)
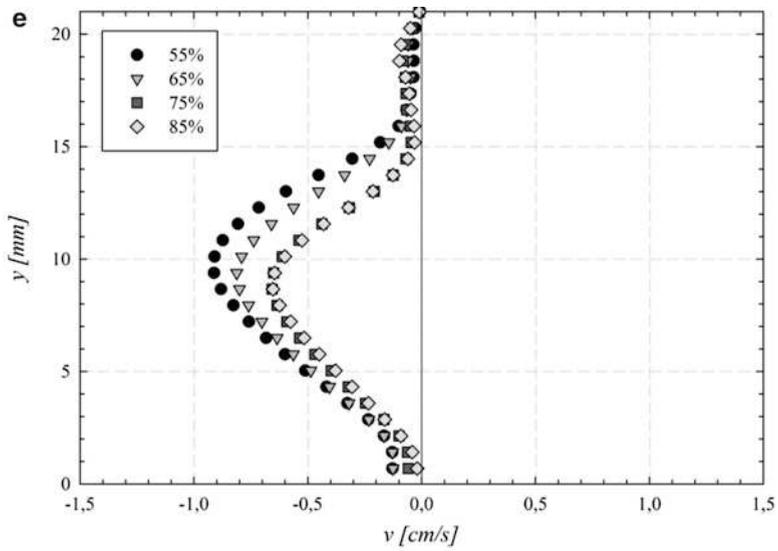
e

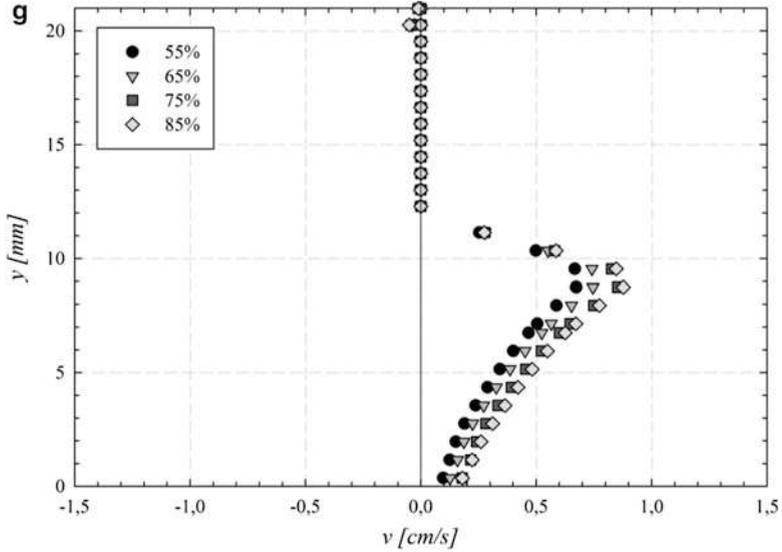

f

Fig. 66.9 (continued)

16

g
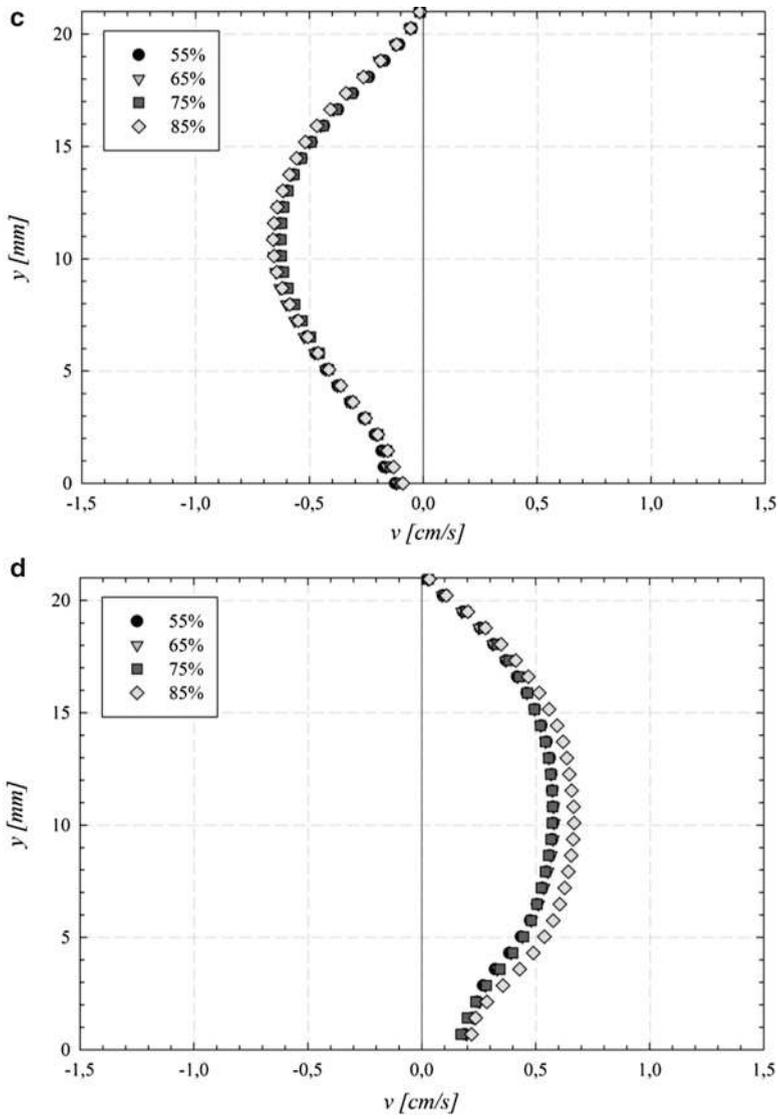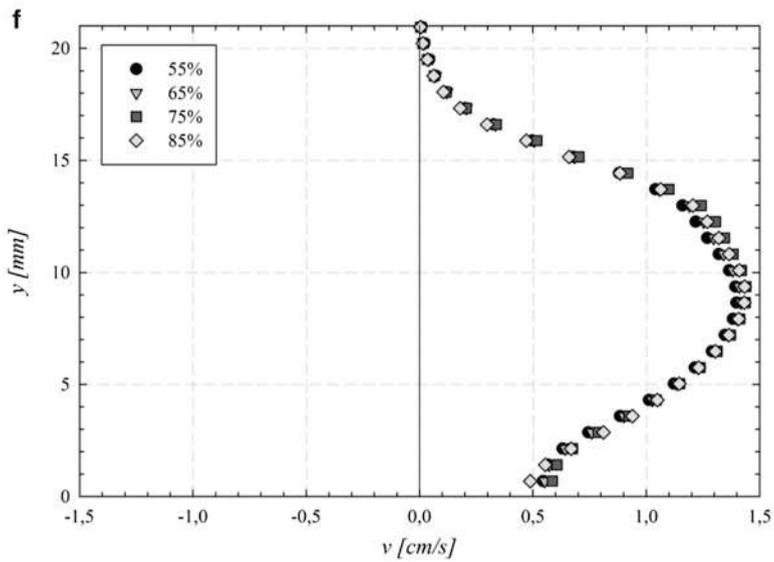
Fig. 66.9 (continued)

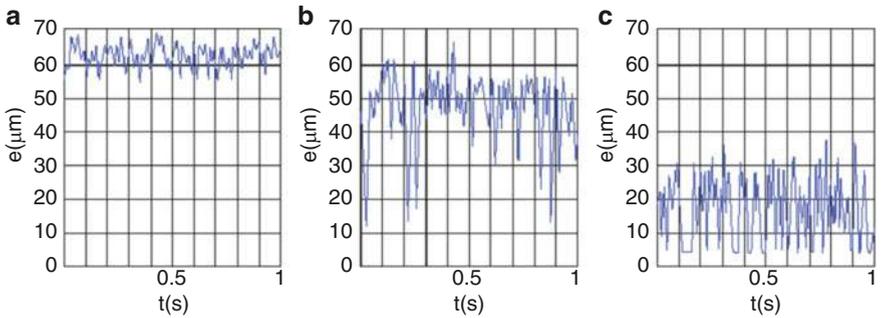**Fig. 66.10** Instant evolution of the liquid film thickness over the channel's lateral wall at the (**a**) liquid/foam interface; (**b**) middle of the lateral wall and (**c**) top side of the lateral wall

From the previous fields, the profiles of the wall shear stress over the later wall along the length of the test channel were extracted and they are displayed in Fig. 66.13. The maximum value is obtained at both upstream and downstream of the singularity where the flow is in a one-dimensional regime with a mean velocity of 1.75 cm/ and at the top of the channel where the liquid film presents its minimal value (5 μm). By moving closer to the singularity, the velocity affects the wall shear stress, and despite having smaller thickness at the top of the wall the maximum stress is created near the maximum values of velocities (4 cm/s) towards the middle, between the fence and the
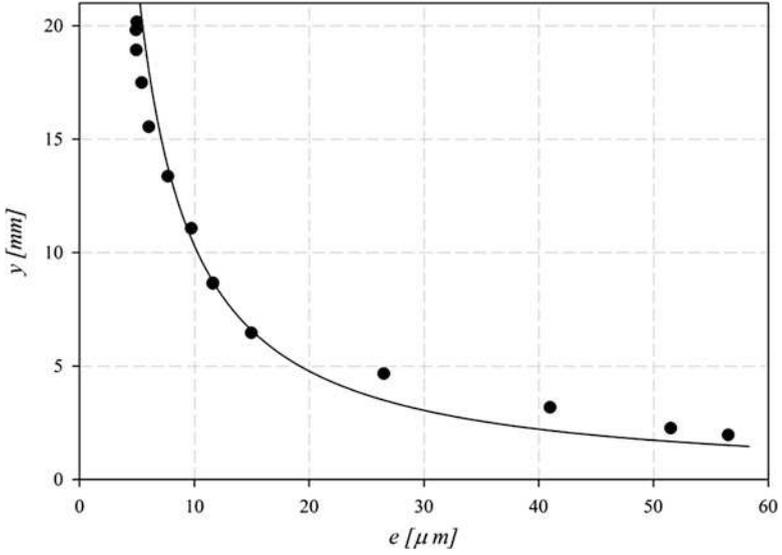
Fig. 66.11 Evolution of the average liquid film thickness along the lateral wall of the channel
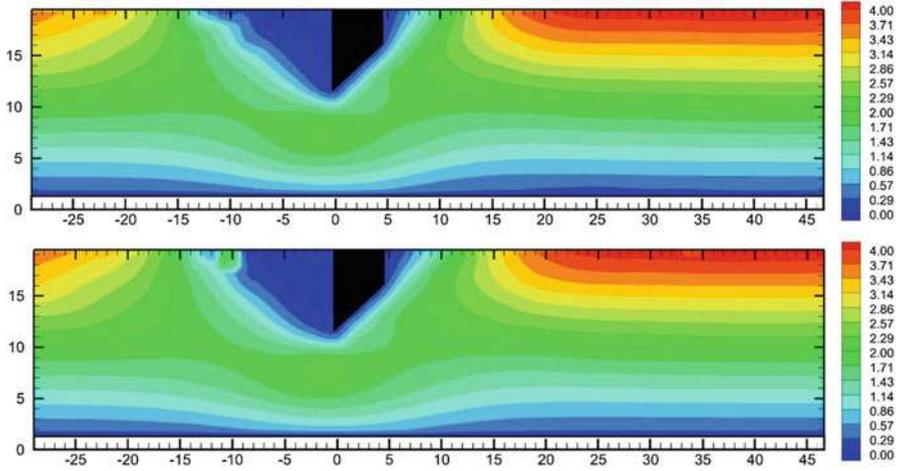

Fig. 66.12 Wall shear stress [Pa] fields for $\beta = 55\,\%$ (*top*) and $\beta = 85\,\%$ (*bottom*)

bottom of the channel. In this region a deviation of around 5 % is noted for the void fraction difference.
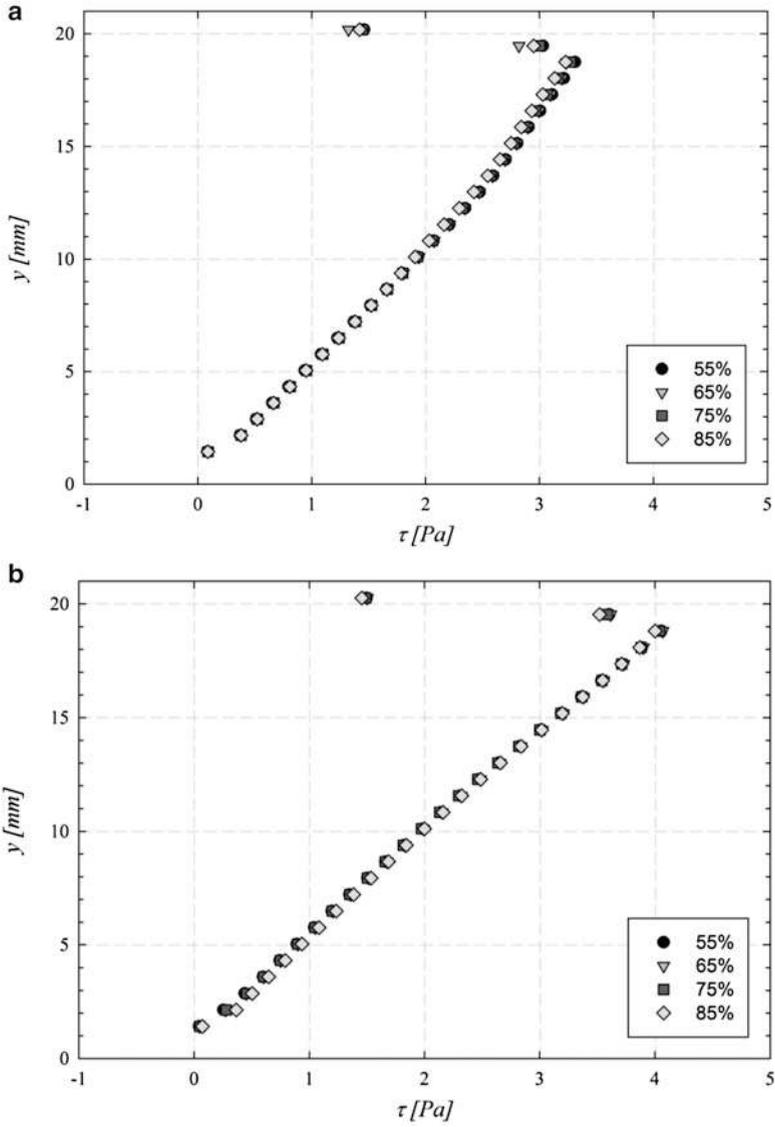
Fig. 66.13 "τ" [Pa] profiles at (**a**) $x = -25$, (**b**) $x = 25$, (**c**) $x = -15$, (**d**) $x = 15$, (**e**) $x = -5$, (**f**) $x = 5$ and (**g**) $x = 0$
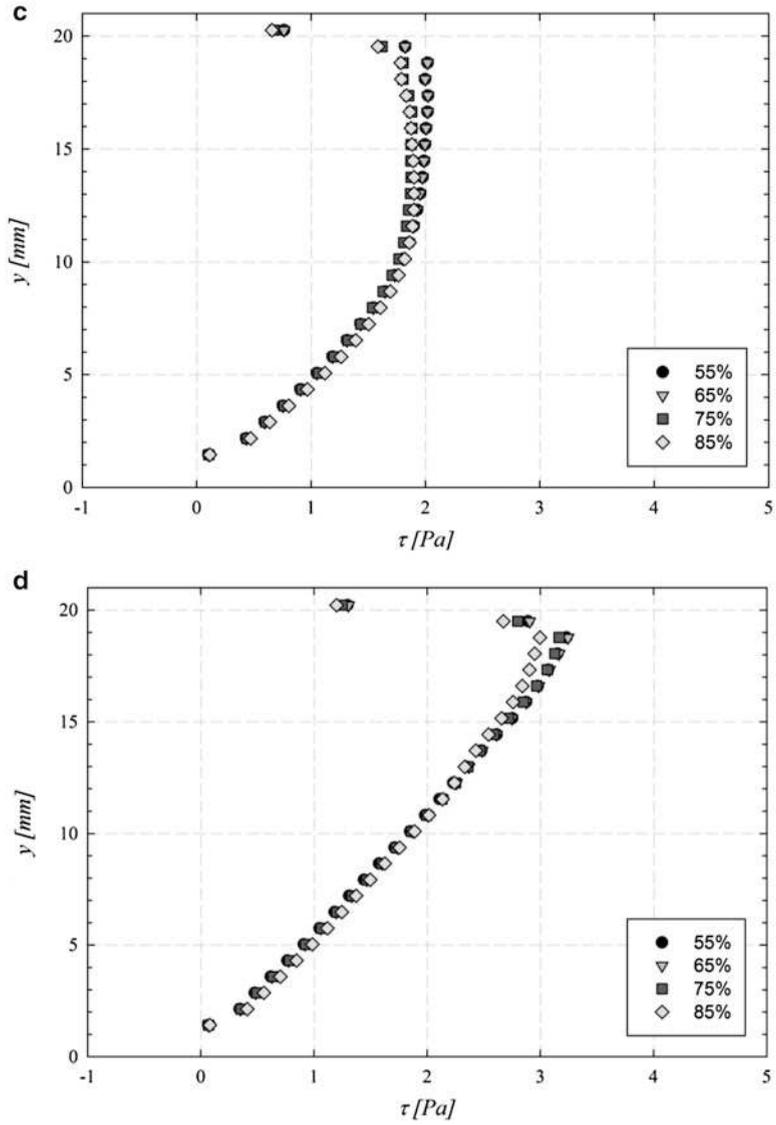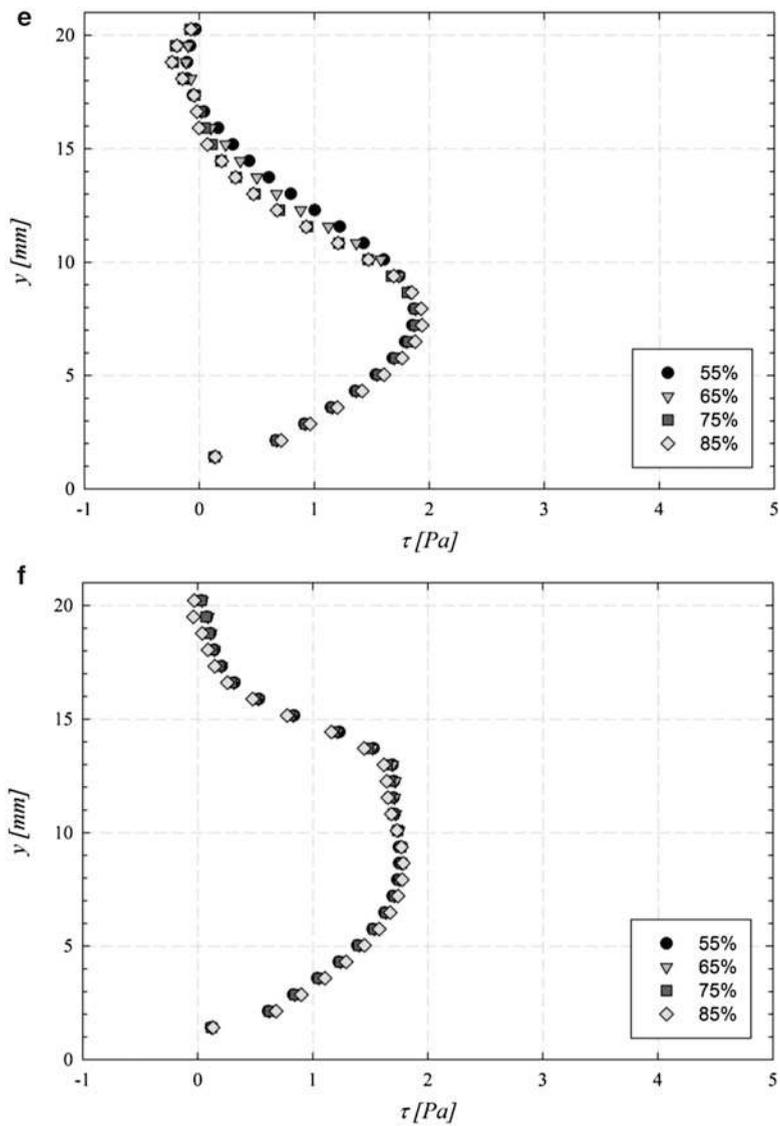
c

d

Fig. 66.13 (continued)
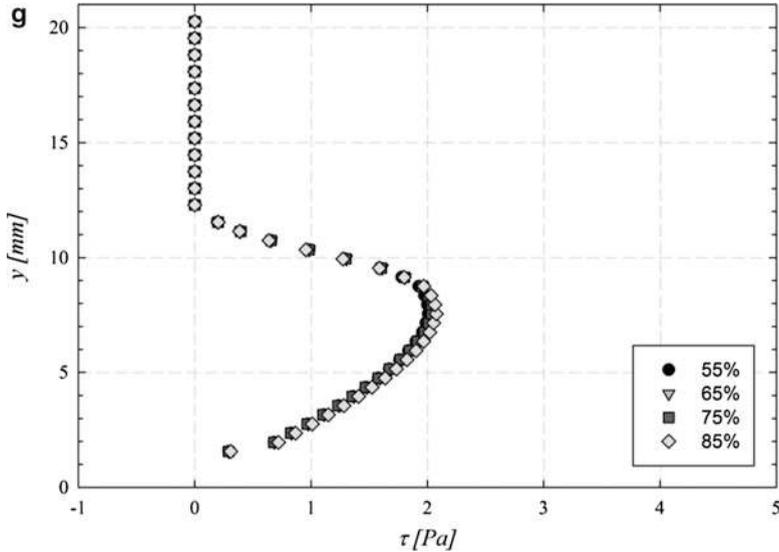
Fig. 66.13 (continued)

21

Fig. 66.13 (continued)

66.5 Conclusions

In this study, we characterize and analyze the velocity fields, liquid film thickness and wall shear stress of an aqueous foam flow with a mean velocity of 1.75 cm/s and void fractions of 55, 65, 75, and 85 %. The mean goal was to attack the two main problems of any foam flow inside a canalization, its rheological and stability properties. The measurements were made over an aqueous foam flowing through a fence with the PIV and conductimetry methods. The results put into evidence the complexity of this flow. The rheological and stability properties are extremely sensitive to the condition of the flow and its surroundings.

The singularity considerably changes the foam flow structure reorganization in its vicinity with an axial acceleration when approaching the fence and deceleration when exiting this one. The dry foam tends to move faster, therefore more shear, in the axial direction than the wet foam. For the vertical velocity component, the gravity and the foam density play a major role in the behavior. When the negative, or downward, movement sets in the wet foam (denser) tends to accelerate more than the dry foam. In the opposite case (upward or positive movement) is the dryer one that moves faster towards the top of the channel.

The obtaining of the liquid film at the lateral wall, with the conductimetry method, allowed the estimation of the wall shear stress. Despite the difference of void fraction, both the liquid film thickness evolution and the wall shear stress do not suffer any important change in their behaviour. Due to drainage forces, the maximum values for the liquid film thickness over the lateral wall were found at the

bottom of the channel and the minimum at the top. The axial velocity does not have a big impact over the maximum value of the wall shear stress. This one is inversely proportionally to the liquid film thickness. The bigger stress is obtained away from the fence, where the foam flow presents one uniform axial component, near the top of the channel, for the smaller thickness. Close to the singularity the axial velocity influences the wall shear stress and a small difference between the dry and wet foam can be noted.

If foam flow can teach something is that problems need to be seen from both the macroscopic and the microscopic points of view. In a foam, the distribution of molecular particles inside the liquid films can change the rheological properties of the whole. The same approach needs to be taken in all subjects concerning energy and its efficiency. Even small changes in a system can improve its performance. Foam flows present complex properties but once they are understood the possibilities are infinite. This study is one step closer in understanding those properties and improving the efficiency of foams used in some industrial processes.

References

1. Plateau JAF (1861) Mem Acad Roy Sci Belg vol. 33. 5th and 6th Series
2. Weaire D, Hutzler S (1999) The physics of foams. Clarendon, Oxford
3. Durian DJ, Weitz DA, Pine DJ (1990) Dynamics and coarsening in three-dimensional foams. J Phys Condens Matter 2:433–436
4. Hutzler S, Saadatfar M, van der Net A, Weaire D, Cox S (2008) The dynamics of a topological change in a system of soap films. Colloids Surf A Physicochem Eng Asp 323:123–131
5. Bikerman JJ (1973) Foams. Springer, New York
6. Weaire D (2008) The rheology of foam. Curr Opin Colloid Interface Sci 13(3):171–176
7. Tisné P, Aloui F, Doubliez L (2003) Analysis of wall shear stress in wet foam flows using the electrochemical method. Int J Multiphase Flow 29(5):841–854
8. Marze S, Langevin D, Saint-Jalmes A (2008) Aqueous foam slip and shear regimes determined by rheometry and multiple light scattering. J Rheol 52:1091
9. Aloui F, Madani S (2007) Wet foam flow under a fence located in the middle of a horizontal duct of square section. Colloids Surf A Physicochem Eng Asp 309:71–86
10. Blondin E, Doubliez L (2002) Particle imaging velocimetry of a wet aqueous foam with an underlying liquid film. Exp Fluids 32(3):294–301
11. Aloui F, Madani S (2008) Experimental investigation of a wet foam flow through a horizontal sudden expansion. Exp Thermal Fluid Sci 32:905–926
12. Tisné P, Doubliez L, Aloui F (2004) Determination of the slip layer thickness for a wet foam flow. Colloids Surf A Physicochem Eng Asp 246:21–29